New Manganese(II) Azido Coordination Polymers with Nicotinic/Isonicotinic Acids as Coligands: Synthesis, Structure, and Magnetic Properties

Qian Yang, Jiong-Peng Zhao, Bo-Wen Hu, Xiao-Feng Zhang, and Xian-He Bu*

Department of Chemistry and TKL of Metal- and Molecule-based Material Chemistry, Nankai University, Tianjin 300071, China

The reactions of Mn^{II} ions with azido ligands in the presence of nicotinic/isonicotinic acids gave two manganese(II) azido coordination polymers, $[Mn_3(L^1)_2(N_3)_4]_n \cdot nH_2O$ (**1**) and $[Mn_2(L^2)(N_3)_3]_n$ (**2**), where L^1 = nicotinate and L^2 = isonicotinate, with different topological structures. Complex **1** consists of 2D azido–Mn^{II} planes, which is further linked by L^1 to form a 3D framework with unprecedented 3,6-connected 4-nodal net topology, and complex **2** presents an unprecedented 3,4,6-connected 6-nodal 3D azido–Mn^{II} structure with L^2 as the coligand. Magnetic susceptibility measurements reveal dominant antiferromagnetic coupling existing in **1** and **2**. Complex **1** is a spin-competitive system and enters into a weak ferromagnetic-to-magnetic phase transition at the critical temperature of 6 K due to spin canting. Complex **2** is an antiferromagnet and exhibits field-induced spin-flop behavior.

Introduction

In the last few decades, the design and synthesis of magnetic coordination polymers with peculiar structure and potential application have become a focus of intense research activities in the fields of coordination and material chemistry.[1] The key to designing such materials is to select a bridging ligand that can effectively mediate the magnetic coupling and construct novel structures.[2] As a bridging ligand, an azido anion displaying multiple bridging modes and various magnetic exchange pathways between metal ions has been well used in the preparation of molecular magnetic materials.[3] It is well-known that an azido anion can link metal ions in μ-1,1 (end-on, EO), μ-1,3 (end-to-end, EE), μ-1,1,3, or still other modes, yielding various discrete, one-, two- (2D), or three-dimensional (3D) species with specific topologies.[4] In general, the EO mode shows ferromagnetic (FM) exchange interactions, while the EE mode affords antiferromagnetic (AF) exchange between the metal ions,[5] and other mixed azido bridging modes also give interesting magnetic properties.[6]

In recent years, the metal azido derivatives have provided a number of excellent structures and magnetic properties such as FM EO chains,[4b,7] AF EE chains,[8] and alternating FM/AF systems[9] due to alternating EE/EO bridges. 2D layers with EE bridges with AF coupling[10] and also alternating EE/EO systems,[11] which magnetically show alternating FM/AF

*To whom correspondence should be addressed. E-mail: buxh@nankai.edu.cn. Tel: +86-22-23502809. Fax: +86-22-23502458.

(1) (a) Kahn, O. *Molecular Magnetism*; VCH: Weinheim, Germany, 1993. (b) Maji, T. K.; Mukherjee, P. S.; Mostafa, G.; Mallah, T.; Cano-Boquera, J.; Chaudhuri, N. R. *Chem. Commun.* **2001,** 1012. (c) Miller, J. S.; Drillon, M. *Magnetism: Molecules to Materials*; Willey-VCH: Weinheim, Germany, 2001−2005.(d) Du, M.; Bu, X.-H.; Guo, Y.-M.; Ribas, J. *Chem.—Eur. J.* **2004,** *10,* 1345.

(2) (a) Ribas, J.; Escuer, A.; Monfort, M.; Vicente, R.; Cortés, R.; Lezama, L.; Rojo, T. *Coord. Chem. Rev.* **1999,** *193−195,* 1027. (b) Escuer, A.; Aromí, G. *Eur. J. Inorg. Chem.* **2006,** 4721. (c) Wang, X.-Y.; Wang, Z.-M.; Gao, S. *Chem. Commun.* **2008,** 281.

(3) (a) Shen, Z.; Zuo, J.-L.; Gao, S.; Song, Y.; Che, C.-M.; Fun, H.-K.; You, X.-Z. *Angew. Chem., Int. Ed.* **2000,** *39,* 3633. (b) Monfort, M.; Resino, I.; Ribas, J.; Stoeckli-Evans, H. *Angew. Chem., Int. Ed.* **2000,** *39,* 191. (c) Zeng, Y.-F.; Hu, X.; Liu, F.-C.; Bu, X.-H. *Chem. Soc. Rev.* **2009,** *38,* 469.

(4) (a) Ge, C.-H.; Cui, A.-L.; Ni, Z.-H.; Jiang, Y.-B.; Zhang, L.-F.; Ribas, J.; Kou, H.-Z. *Inorg. Chem.* **2006,** *45,* 4883. (b) Liu, T.-F.; Fu, D.; Gao, S.; Zhang, Y.-Z.; Sun, H.-L.; Su, G.; Liu, Y.-J. *J. Am. Chem. Soc.* **2003,** *125,* 13976. (c) Wang, X.-Y.; Wang, L.; Wang, Z.-M.; Su, G.; Gao, S. *Chem. Mater.* **2005,** *17,* 6369. (d) Gao, E.-Q.; Wang, Z.-M.; Yan, C.-H. *Chem. Commun.* **2003,** 1748.

(5) Charlot, M. F.; Kahn, O.; Chaillet, M.; Larrieu, C. *J. Am. Chem. Soc.* **1986,** *108,* 2574.

(6) (a) Manson, J. L.; Arif, A. M.; Miller, J. S. *Chem. Commun.* **1999,** 1479. (b) Hao, X.; Wei, Y.; Zhang, S.-W. *Chem. Commun.* **2000,** 2271. (c) Chen, H.-J.; Mao, Z.-W.; Gao, S.; Chen, X.-M. *Chem. Commun.* **2001,** 2320. (d) Gao, E.-Q.; Bai, S.-Q.; Wang, C.-F.; Yue, Y.-F.; Yan, C.-H. *Inorg. Chem.* **2003,** *42,* 8456.

(7) (a) Bai, S.-Q.; Gao, E.-Q.; He, Z.; Fang, C.-J.; Yue, Y.-F.; Yan, C.-H. *Eur. J. Inorg. Chem.* **2006,** *2,* 407. (b) Yue, Y.-F.; Gao, E.-Q.; Fang, C.-J.; Zheng, T.; Liang, J.; Yan, C.-H. *Inorg. Chem.* **2008,** *8,* 3295.

(8) (a) Escuer, A.; Vicente, R.; Goher, M. A. S.; Mautner, F. A. *Inorg. Chem.* **1998,** *37,* 782. (b) Liu, X.-T.; Wang, X.-Y.; Zhang, W.-X.; Cui, P.; Gao, S. *Adv. Mater.* **2006,** *18,* 2852.

(9) (a) Abu-Youssef, M. A. M.; Escuer, A.; Goher, M. A. S.; Mautner, F. A.; Vicente, R. *Eur. J. Inorg. Chem.* **1999,** 687. (b) Mukherjee, P. S.; Maji, T. K.; Mostafa, G.; Mallah, T.; Chaudhuri, N. R. *Inorg. Chem.* **2000,** *39,* 5147.

(10) (a) Escuer, A.; Vicente, R.; Goher, M. A. S.; Mautner, F. A. *J. Chem. Soc., Dalton Trans.* **1997,** 4431. (b) Li, R.-Y.; Wang, X.-Y.; Liu, T.; Xu, H.-B.; Zhao, F.; Wang, Z.-M.; Gao, S. *Inorg. Chem.* **2008,** *47,* 8134.

(11) (a) Goher, M. A. S.; Al-Salem, N. A.; Mautner, F. A. *J. Coord. Chem.* **1998,** *44,* 119. (b) Wang, X.-Y.; Wang, L.; Wang, Z.-M.; Gao, S. *J. Am. Chem. Soc.* **2006,** *128,* 674.

coupling, have been characterized. Regular 3D AF compounds have also been described with only EE azido bridges.[12] However, it is still hard to exactly forecast which coordination mode azido ligand will be adopted to coordinate the transition-metal center in a detailed system.[2a]

On the other hand, an azido bridging ligand can be further utilized to cooperate with the ancillary bridging ligand to construct transition-metal coordination polymer magnetic materials. The heterocyclic carboxylic acid ligands with N and O donors always offer great potential for constructing architectures.[13,14] Among aromatic carboxylic acids, nicotinic/isonicotinic acids have a conjugated structural character, and they are quite interesting candidates in the construction of extended structures because they are unsymmetrical divergent ligands. They can link two or three metal centers by coordinating to a metal ion with the N atom and to other metal ion(s) with one or two carboxylate O atoms. Although a number of transition metal−nicotinate/isonicotinate−azido complexes have so far been documented,[15] the Mn^{II}−nicotinate/isonicotinate−azido coordination polymers are few, especially the azido anions linking the metal ions to form a 3D structure directly.[6c,16]

In this work, choosing the nicotinic and isonicotinic acids to be the coligands, we report the synthesis, structural characterization, and magnetic properties of two novel azido−Mn^{II} coordination polymers, $[Mn_3(L^1)_2(N_3)_4]_n \cdot nH_2O$ (**1**) and $[Mn_2(L^2)(N_3)_3]_n$ (**2**), where L^1 = nicotinate and L^2 = isonicotinate. Complex **1** consists of 2D azido−Mn^{II} planes further linked by L^1, forming a 3D framework, and **1** exhibits a brilliant 3,6-connected 4-nodal net topology with Schläfli notation $\{4^2.6\}4\{4^3\}2\{4^4.6^2.8^6.10^3\}\{4^5.6^4.8^6\}2$. Complex **2** presents an unprecedented 3,4,6-connected 6-nodal 3D azido−Mn^{II} structure with a coligand L^2, and its Schläfli symbol is $\{4.5.6\}2\{4.5^2\}2\{4^3.5^2.7\}2\{4^3.5^4.6^5.7^2.8\}2\{4^4.5^6.6^2.7^3\}$-$\{5^4.6^4.7^4.9^3\}$. The magnetic study reveals that, in **1** and **2**, there exists AF coupling between Mn^{II} ions with the μ-1,1,3 or μ-1,3 mode and the μ-1,1,3 mode azido anions. In addition, complex **1** is a spin-competitive system, but **1** has a FM-to-magnetic phase transition at the critical temperature of 6 K due to spin canting. Complex **2** is an antiferromagnet and exhibits a field-induced spin-flop behavior.

(12) (a) Han, S.; Manson, J. L.; Kim, J.; Miller, J. S. *Inorg. Chem.* **2000**, *39*, 4182. (b) Escuer, A.; Vicente, R.; Mautner, F. A.; Goher, M. A. S.; Abu-Youssef, M. A. M. *Chem. Commun.* **2002**, 64.

(13) (a) Zhang, X.-M.; Tong, M.-L.; Chen, X.-M. *Angew. Chem., Int. Ed.* **2002**, *41*, 1029. (b) Ciurtin, D. M.; Smith, M. D.; zur Loye, H. C. *Chem. Commun.* **2002**, 74. (c) Ciurtin, D. M.; Smith, M. D.; zur Loye, H. C. *Dalton Trans.* **2003**, 1245. (d) Lu, J.-Y. *Coord. Chem. Rev.* **2003**, *246*, 327. (e) Humphrey, S. M.; Wood, P. T. *J. Am. Chem. Soc.* **2004**, *126*, 13236. (f) Ghosh, S. K.; Bharadwaj, P. K. *Inorg. Chem.* **2005**, *44*, 3156.

(14) (a) Fan, J.; Sun, W.-Y.; Okamura, T.; Zheng, Y.-Q.; Sui, B.; Tang, W.-X.; Ueyama, N. *Cryst. Growth Des.* **2004**, *4*, 579. (b) Sun, C.-Y.; Zheng, X.-J.; Gao, S.; Li, L.-C.; Jin, L.-P. *Eur. J. Inorg. Chem.* **2005**, 4150. (c) Eubank, J. F.; Walsh, R. D.; Eddaoudi, M. *Chem. Commun.* **2005**, 2095. (d) Zhang, M.-B.; Zhang, J.; Zhang, S.-T.; Yang, G.-Y. *Angew. Chem., Int. Ed.* **2005**, *44*, 1385. (e) Wang, Y.-T.; Tang, G.-M.; Wu, Y.; Qin, X.-Y.; Qin, D.-W. *J. Mol. Struct.* **2007**, *831*, 61. (f) Mahata, P.; Ramya, K. V.; Natarajan, S. *Chem.—Eur. J.* **2008**, *14*, 5839.

(15) (a) Liu, F.-C.; Zeng, Y.-F.; Li, J.-R.; Bu, X.-H.; Zhang, H.-J.; Ribas, J. *Inorg. Chem.* **2005**, *44*, 7298. (b) Liu, F.-C.; Zeng, Y.-F.; Zhao, J.-P.; Hu, B.-W.; Sañudo, E. C.; Ribas, J.; Bu, X.-H. *Inorg. Chem.* **2007**, *46*, 7698. (c) Liu, F.-C.; Zeng, Y.-F.; Jiao, J.; Bu, X.-H.; Ribas, J.; Batten, S. R. *Inorg. Chem.* **2006**, *45*, 2776. (d) Liu, F.-C.; Zeng, Y.-F.; Jiao, J.; Li, J.-R.; Bu, X.-H.; Ribas, J.; Batten, S. R. *Inorg. Chem.* **2006**, *45*, 6129.

(16) Cheng, L.; Zhang, W.-X.; Ye, B.-H.; Lin, J.-B.; Chen, X.-M. *Eur. J. Inorg. Chem.* **2007**, 2668.

Experimental Section

General Methods. All starting materials for synthesis were commercially available and were used as purchased. Elemental analysis of C, H, and N was carried out with a Perkin-Elmer 240C analyzer. IR spectra were measured on a Tensor 27 OPUS (Bruker) FT-IR spectrometer with KBr pellets. The powder X-ray diffraction (PXRD) was recorded on a Rigaku D/Max-2500 diffractometer at 40 kV and 100 mA for a copper-target tube and a graphite monochromator. Simulation of the PXRD spectra was carried out by the single-crystal data and diffraction-crystal module of the Mercury (Hg) program available free of charge via the Internet at http://www.iucr.org. Magnetic data were collected using crushed crystals of the sample on a Quantum Design MPMS-XL SQUID magnetometer. The data were corrected using Pascal's constants to calculate the diamagnetic susceptibility, and an experimental correction for the sample holder was applied.

Synthesis. $[Mn_3(L^1)_2(N_3)_4]_n \cdot nH_2O$ (**1**). **1** was hydrothermally synthesized under autogenous pressure. A mixture of $MnCl_2 \cdot 4H_2O$ (0.5 mmol), HL^1 (0.5 mmol), NaN_3 (3 mmol), and CH_3OH (10 mL) was sealed in a Teflon-lined autoclave and heated to 140 °C. After the reaction vessel was maintained for 48 h, it was cooled to room temperature in 24 h. Pure yellow-green crystals were collected with ∼40% yield based on HL^1. Anal. Calcd for $C_{12}H_{10}Mn_3N_{14}O_5$: C, 24.22; H, 1.69; N, 32.95. Found: C, 24.95; H, 1.79; N, 31.42. FT-IR (KBr pellets, cm^{-1}): 3134, 2106, 2073, 1614, 1585, 1568, 1406, 754, 698.

$[Mn_2(L^2)(N_3)_3]_n$ (**2**). Lawn-green single crystals of **2** suitable for X-ray analysis were obtained by a method similar to that described for **1**, except HL^2 was used as the ligand. Yield: ∼30% based on HL^2. Anal. Calcd for $C_6H_4Mn_2N_{10}O_2$: C, 20.13; H, 1.13; N, 39.12. Found: C, 20.53; H, 1.32; N, 39.29. FT-IR (KBr pellets, cm^{-1}): 3413, 2102, 2086, 1616, 1548, 1494, 1398, 775, 688.

Caution! *Azido−metal complexes are potentially explosive; only a small amount of material should be prepared with care.*

X-ray Data Collection and Structure Determinations. Single-crystal XRD data for complexes **1** and **2** were collected on a Scx-Mini diffractometer at 293(2) K with Mo Kα radiation (λ = 0.710 73 Å) by an ω scan mode. The program *SAINT*[17] was used for integration of the diffraction profiles. All of the structures were solved by direct methods using the *SHELXS* program of the *SHELXTL* package and refined by full-matrix least-squares methods with *SHELXL* (semiempirical absorption corrections were applied using the *SADABS* program).[18] Metal atoms in each complex were located from the *E* maps, and other non-H atoms were located in successive difference Fourier syntheses and refined with anisotropic thermal parameters on F^2. The H atoms of the ligands were generated theoretically onto specific atoms and refined isotropically with fixed thermal factors. Detailed crystallographic data are summarized in Table 1.

Results and Discussion

Crystal Structure of the Complexes. Complex **1** crystallizes in the triclinic space group $P\bar{1}$. In the lattice, there are two types of crystallographically independent Mn^{II} ions: Mn1 and Mn2. The asymmetric unit of this complex consists of half of a Mn1 ion and one Mn2 ion, two azido anions, one L^1 ligand, and half of a water molecule. The Mn1 ion is located at an inversion center with an octahedral coordination environment in which the equatorial plane is made up of four N atoms from four azido anions

(17) *SAINT Software Reference Manual*; Bruker AXS: Madison, WI, 1998.
(18) Sheldrick, G. M. *SHELXTL NT Version 5.1. Program for Solution and Refinement of Crystal Structures*; University of Göttingen: Göttingen, Germany, 1997.

Table 1. Crystal Data and Structure Refinement Parameters for Complexes **1** and **2**

	1	**2**
chemical formula	$C_{12}H_{10}Mn_3N_{14}O_5$	$C_6H_4Mn_2N_{10}O_2$
fw	595.16	358.07
space group	$P\bar{1}$	$P2_1/c$
$a/\text{Å}$	6.9439(14)	11.676(2)
$b/\text{Å}$	7.8714(16)	7.0135(14)
$c/\text{Å}$	9.840(2)	14.839(3)
$\alpha/\deg$	103.45(3)	90
$\beta/\deg$	98.74(3)	102.06(3)
$\gamma/\deg$	98.23(3)	90
$V/\text{Å}^3$	508.02(18)	1188.3(4)
Z	1	4
$D/\text{g cm}^{-3}$	1.945	2.002
μ/mm^{-1}	1.898	2.145
T/K	293	293
$R^a/R_w{}^b$	0.0312/0.0769	0.0359/0.0592

$$^a R = \sum ||F_o| - |F_c||/\sum |F_o|. \quad {}^b R_w = [\sum [w(F_o{}^2 - F_c{}^2)^2]/\sum w(F_o{}^2)^2]^{1/2}.$$

and the axial sites are occupied by two O atoms from two $\mathbf{L^1}$ ligands (Figure 1a). Mn1 has two pairs of Mn1−N distances of 2.278 and 2.288 Å, and the distance of Mn1−O is 2.092 Å (see Table S1 in the Supporting Information). Mn2 lies in a distorted octahedral coordination sphere. There are four N atoms from four azido anions and one N atom and one O atom from the $\mathbf{L^1}$ ligand coordinating with the Mn2 ion. The Mn2−N/O distances are in the normal range of 2.099−2.323 Å. There are two kinds of azido anions in the asymmetric unit. They take the μ-1,1,3 mode linking three Mn^{II} ions. The distances of the Mn^{II} ions bridged by the azido anion are Mn1···Mn2B = 4.012 Å, Mn1··· Mn2A = 5.401 Å, Mn1···Mn2 = 6.333 Å, Mn2A··· Mn2B = 5.346 Å, and Mn2···Mn2A = 3.567 Å. The carboxylate group bridges two types of Mn^{II} ions with the *syn,syn* mode. The 3D structure can be described as follows: first, the azido anions take the μ-1,1,3 mode with the angles Mn1−N3A−Mn2B = 123.43° and Mn2− N4−Mn2A = 103.12° linking two types of Mn^{II} ions and forming a 2D plane (Figure 1b). Then, these planes are connected via $\mathbf{L^1}$ ligands, forming a 3D framework (Figure 1c).

As described above, the azido ligand shows a μ-1,1,3 bridging mode and connects three Mn^{II} ions, while the nicotinic acid ligand coordinates to three Mn^{II} ions, one each per O or N atom. The Mn^{II} ion coordinates to four azido ligands and two $\mathbf{L^1}$ ligands. Thus, from a topological viewpoint, the Mn^{II} ions act as 6-connected nodes and the $\mathbf{L^1}$ ligands and azido ligands act as 3-connected nodes. The overall 3,6-conneted 3D network is shown in Figure 1d. To the best of our knowledge, this 3,6-connected net with the Schläfli symbol of $\{4^2.6\}4\{4^3\}2\{4^4.6^2.8^6.10^3\}$ $\{4^5.6^4.8^6\}2$ is unprecedented.

Complex **2** crystallizes in the monoclinic space group $P2_1/c$ consisting of a 3D supramolecular network formed by the Mn^{II} ion, μ-1,1,3-azido, μ-1,3-azido, and the $\mathbf{L^2}$ ligand as the coligand. There are three types of crystallographically independent Mn^{II} ions in the lattice: Mn1, Mn2, and Mn3. In the asymmetric unit of complex **2**, there is one Mn1, half of a Mn2 ion, half of a Mn3 ion, three azido anions, and one $\mathbf{L^2}$ ligand. The three types of Mn^{II} ions are located at the inversion centers with an octahedral coordination environment (Figure 2a). Mn1 and Mn2 ions are both coordinated by two O atoms from

$\mathbf{L^2}$ ligands and four N atoms from azido anions. There are six N atoms coordinating with the Mn3 ion. Two of them come from two $\mathbf{L^2}$ ligands, and others come from four azido anions. The Mn−N/O distances are in the normal range of 2.144−2.320 Å (see Table S1 in the Supporting Information). There are three kinds of azido anions in the asymmetric unit. Two of them take the μ-1,1,3 mode linking three Mn^{II} ions and one of them takes the μ-1,3 mode linking two Mn^{II} ions. The angles of Mn1−N8−Mn2 and Mn1B−N4B−Mn2 are 117.04° and 120.90°, respectively. The distances of the Mn^{II} ions bridged by the azido anion are Mn1···Mn2 = 3.909 Å, Mn1···Mn3G = 5.866 Å, Mn1···Mn3 = 5.882 Å, Mn1···Mn1K = 6.079 Å, Mn2···Mn1B = 3.932 Å, Mn2···Mn3L = 5.838 Å, and Mn2···Mn1K = 6.065 Å. The carboxylate group bridges two types but three Mn^{II} ions in the μ_3-O,O,O′ mode. The angle of Mn1−O1C−Mn1B is 103.50°. Two types of azido anions link three types of Mn^{II} ions, forming a 3D azido−Mn^{II} net (Figure 2b). Furthermore, the unligated sites of Mn^{II} ions are occupied by the $\mathbf{L^2}$ ligands (Figure 2c). The 3D azido−Mn^{II} structure should be described as follows: first, Mn^{II} ions connected through μ-1,1,3 and μ-1,3 mode azido anions, forming a 2D azido−Mn^{II} layer; which further connected into a rare 3D azido−Mn^{II} net through the other μ-1,1,3 mode azido.[6c,12,19]

Complex **2** contains two kinds of azido anions, a μ-1,1,3 mode linking three Mn^{II} ions, a μ-1,3 mode linking two Mn^{II} ions, one $\mathbf{L^2}$ ligand coordinating to four Mn^{II} ions, and three types of Mn^{II} ions coordinating to two $\mathbf{L^2}$ ligands and four azido ligands. Topologically, the structure is composed of 3-connecting azido anions, 4-connecting $\mathbf{L^2}$ ligands, and 6-connecting Mn^{II} ions. The complicated 3,4,6-connected network is shown in Figure 2d. The Schläfli symbol is $\{4.5.6\}2\{4.5^2\}2\{4^3.5^2.7\}2\{4^3.5^4.6^5.7^2.8\}2\{4^4.5^6.6^2.7^3\}$- $\{5^4.6^4.7^4.9^3\}$.

Magnetic Studies. Magnetic measurements were carried out on crystalline samples of complexes **1** and **2**, whose purity phase was confirmed by PXRD (see Figure S1 in the Supporting Information). The obtained data indicate dominant AF coupling between the Mn^{II} ions in **1** and **2**. However, in the low-temperature region, they show different magnetic behaviors, as discussed below.

The magnetic property of **1** was investigated by solid-state magnetic susceptibility measurements in the 2.0− 300 K range at a field of 2 kOe. The magnetic property of complex **1** in the form of $\chi_m T$ vs T plots is shown in Figure 3a. The value of $\chi_m T$ at 300 K is 10.67 cm^3 K mol^{-1}, which is lower than that expected (13.14 cm^3 K mol^{-1}) for three magnetically isolated high-spin Mn^{II} ions. As the temperature decreases, the value of $\chi_m T$ slowly decreases down to a minimum value of 6.53 cm^3 K mol^{-1} at 55 K and then rises rapidly to a maximum value of 12.00 cm^3 K mol^{-1} at 16 K. Upon a further decrease of the temperature, however, lower than 16 K, the $\chi_m T$ drops rapidly because of the saturation effect. Fitting the data at 75−300 K with the Curie−Weiss law gives C = 13.45 cm^3 K mol^{-1} and θ = −76.67 K for **1**. The C value is consistent with the value (13.1 cm^3 K mol^{-1}) of three noninteracting Mn^{II} ions with g = 2.0. The negative value of θ and the initial decrease of

(19) (a) Goher, M. A. S.; Cano, J.; Journaux, Y.; Abu-Youssef, M. A. M.; Mautner, F. A.; Escuer, A.; Vicente, R. *Chem.—Eur. J.* **2000**, *6*, 778.
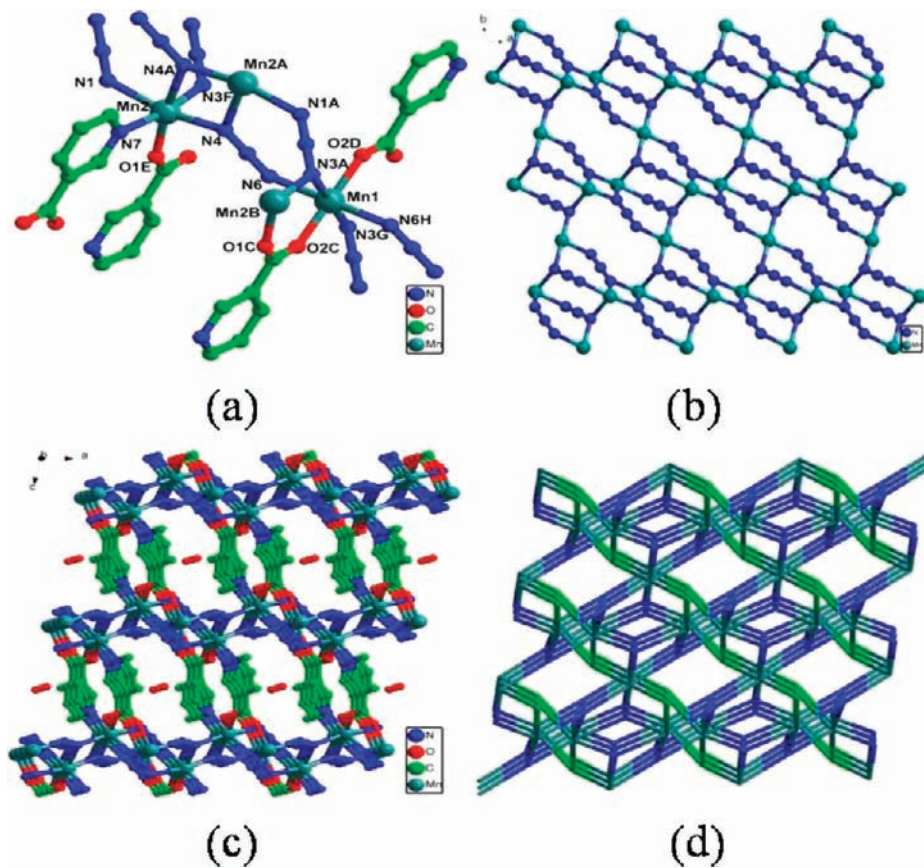
Figure 1. (a) Coordination and linkage modes of the ligands and Mn^{II} ions in **1**. (b) Azido–Mn^{II} 2D plane in **1**. (c) 3D structure of **1** along the *b* direction. (d) Topology network of **1**.
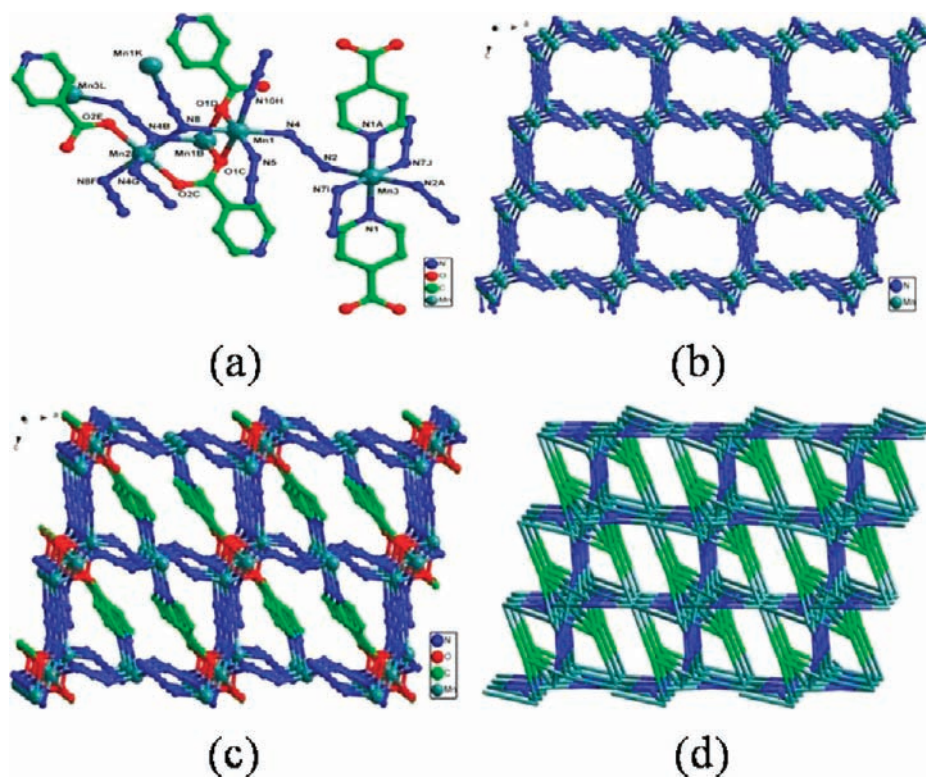

Figure 2. (a) Coordination and linkage modes of the ligands and Mn^{II} ions in **2**. (b) Azido–Mn^{II} 3D net in **2**. (c) 3D structure of **2** along the *b* direction. (d) Topology network of **2**.
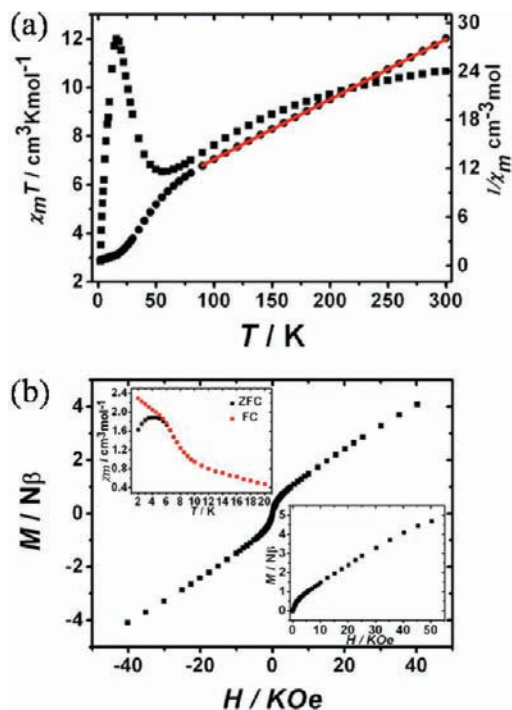
Figure 3. (a) $\chi_m T$ vs T plots of **1** (■) at 2 kOe and $1/\chi_m$ vs T plots of **1** (●). The red solid line is the best fit to the Curie–Weiss law. (b) Hysteresis loop for **1** per three Mn^{II} ions. Insets: The magnetization vs field plots at 2.0 K and ZFC and FC plots of **1**.

$\chi_m T$ should be due to the overall AF coupling between the Mn^{II} ions. The shape of the $\chi_m T$ vs T plots, with its minimum, is typical of ferrimagnetic behavior or spin canting.[1a] However, ferrimagnetic systems usually exhibit less sharp minima. So, taking into account the large number of Mn^{II} networks with similar properties, it should be a spin-canting system. The isothermal field-dependent magnetizations $M(H)$ at 2 K at fields up to 50 kOe (Figure 3b, inset right) were measured for **1**. The field dependence of the magnetization does not follow a Brillouin curve. As shown in Figure 2, M increases quickly at very low field, reaching about 1 Nβ at 2000 Oe, and then increases slowly to 4.45 Nβ at 50 kOe, much less than the common value of 15 Nβ for three Mn^{II} centers, which also suggests the canted AF nature of the interaction between neighboring metal ions. The possibility for long-range order suggested by the sharp peaks in the $\chi_m T$ curves was further investigated by measurement of the zero-field-cooled (ZFC) and field-cooled (FC) magnetizations in the 2–20 K temperature range (Figure 3b, inset left). The ZFC/FC measurements were carried out at a very low field of 20 Oe for **1**. The two curves are superposed at higher temperatures for both fields. They increase abruptly below 10 K and then diverge at around 6 K for **1**. To further probe the long-range ordering in **1**, the alternating-current (ac) magnetic susceptibility measurements were performed with different ac frequencies (Figure S2 in the Supporting Information). Both in-phase $\chi_m{}'$ and out-of-phase $\chi_m{}''$, which were observed in a field of 3.5 Oe oscillating at 100 Hz and 997 Hz, also indicate a canted antiferromagnet with $T_N = 6$ K. Because there are
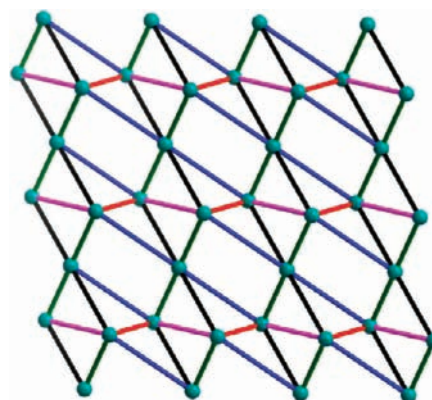
Figure 4. Magnetic network of complex **1** (the lines in different color are the different magnetic passages by azido between Mn^{II} ions).

no disordered components in the system, the slight frequency dependence on $\chi_m{}'$ and $\chi_m{}''$ might be due to the movement of the domain walls.[20] No significant hysteresis was found in **1** at 2 K (Figure 3b).
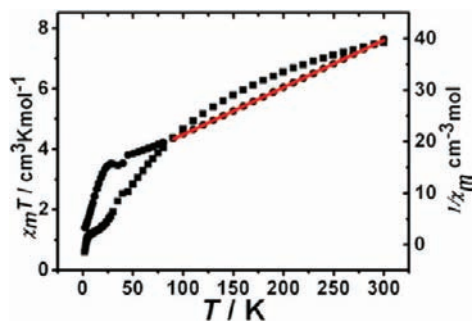
Taking into account the structural features of the compound, further inspection of the magnetic behaviors is worthwhile. Because the exchange interaction through the **L**^{1} ligand can be considered to be negligible, the magnetic net is reduced in complexity because this node can be deleted. On the other hand, the EO azide can mediate antiferromagnetically for the Mn–N–Mn angle 94.1°.[21] In complex **1**, the μ-1,1,3 mode azido anions mediate antiferromagnetically. So, the Mn^{II} ions linking the μ-1,1,3 mode azido all exhibit AF coupling. Thus, we build the net from links (couplings) between Mn^{II} ions via the EE or EO azido anions. This results in a 5,6-connected 2-nodal 2D magnetic network with the topology symbol $\{3^4.4\}2\{3^2.4.3^2.4\}$ (Figures 4 and S3 in the Supporting Information). A triangle of three AF-coupled spins is inherently competitive. In the present complex, Mn$^{II}{}_3$ triangles (connected with black, red, and blue or black, pink, and green lines) share apexes and edges, forming a rectangle (connected with blue and green lines). The resulting 2D lattice represents a novel type of competitive 2D net, which is distinct from other geometrically competitive lattices, where the triangles share corners and edges, as in the well-known triangular and kagóme lattices. In this new lattice, spin competition may also occur on the 6-connected Mn^{II} ions center, as schematized in Figure 4. Experimentally, the degree of competition is identified by the ratio of the Weiss constant to the ordering temperature, $f = |\theta|/T_N$ provided by Ramirez.[22] Competition is present when $f > 1$, where $f > 10$ signifies a strong competition.[23] From the above θ value of −76.67 K and the T_N value of 6 K, an f value of 12.7 is obtained for 1. $f > 10$, indicative of a very strong competition, is observed.

(20) Haase, W.; Wróbel, S. *Relaxation Phenomena: Liquid Crystals, Magnetic Systems, Polymers, High-T$_c$ Superconductors, Metallic Glasses*; Springer-Verlag: New York, 2003.

(21) (a) Villanueva, M.; Mesa, J. L.; Urtiaga, M. K.; Cortés, R.; Lezama, L.; Arriortua, M. I.; Rojo, T. *Eur. J. Inorg. Chem.* **2001**, 1581. (b) Ruiz, E.; Cano, J.; Alvarez, S.; Alemany, P. *J. Am. Chem. Soc.* **1998**, *120*, 11122. (c) Abu-Youssef, M. A. M.; Escuer, A.; Gatteschi, D.; Goher, M. A. S.; Mautner, F. A.; Vicente, R. *Inorg. Chem.* **1999**, *38*, 5716.

(22) (a) Greedan, J. E. *J. Mater. Chem.* **2001**, *11*, 37. (b) Wang, X.-Y.; Sevov, S. C. *Chem. Mater.* **2007**, *19*, 3763. (c) Schiffer, P.; Ramirez, A. P. *Comments Condens. Matter Phys.* **1996**, *18*, 21.

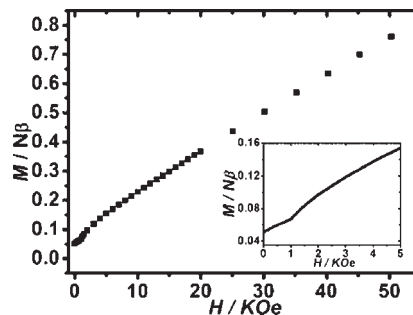(23) Ramirez, A. P. *Annu. Rev. Mater. Sci.* **1994**, *24*, 453.

Figure 5. $\chi_m T$ vs T plots of **2** (■) at 2 kOe and $1/\chi_m$ vs T plots of **2** (●). The red solid line is the best fit to the Curie−Weiss law.

Figure 6. Magnetization vs field plots at 2.0 K of **2**. The inset shows the low-field parts of the magnetization curves at 2.0 K.

The temperature dependences of the magnetic suscept-ibility (χ_m; Figure S4 in the Supporting Information) and its product with temperature ($\chi_m T$; Figure 5) for complex **2** at a field of 2 kOe are shown in Figure 5. The value of $\chi_m T$ at 300 K is 7.52 cm^3 K mol^{-1}, which is lower than that expected (8.76 cm^3 K mol^{-1}) for two magnetically isolated high-spin Mn^{II} ions. As the sample is cooled from room temperature, χ_m first increases smoothly to reach a rounded maximum of 0.065 cm^3 mol^{-1} at about 35 K, then decreases slightly to 0.063 cm^3 mol^{-1} at about 28 K, and finally increases rapidly to 0.303 cm^3 mol^{-1} at 2.0 K. On the other hand, $\chi_m T$ first decreases smoothly upon cooling to a value of 2.59 cm^3 K mol^{-1} at 45 K, and then after a slight decrease to a value of 2.54 cm^3 K mol^{-1} at 40 K, it decreases rapidly again upon further cooling to 2.0 K. Fitting of the $\chi_m^{-1} - T$ at 90−100 K using the Curie−Weiss law $\chi_m = C/(T - \theta)$ gives the Curie con-stant $C = 10.89$ cm^3 K mol^{-1} and the Weiss constant $\theta = -132.98$ K. The negative θ value also supports the pre-sence of an overall AF interaction in complex **2**. A peak at ca. 35 K in the $\chi_m - T$ plots is characteristic of a phase transition to an AF-ordered structure. However, the magnetic behavior of **2** is more complicated in low field. As shown in Figure S5, inset right, in the Supporting Information, upon exposure to a magnetic field of 20 Oe in the 30−45 K range, the value of χ_m increases to a maximum at ca. 36 K and finally decreases upon further cooling. Interestingly, the magnetic behavior of **2** is highly dependent on the applied field, and the values of the peak around 35 K in the $\chi_m - T$ curve become low as the field increases (Figure S5, inset, in the Supporting Informa-tion). These features suggest the occurrence of a field-induced spin-flop transition.[24]

Further experimental evidence for the field-induced spin-flop transition in **2** comes from the field-dependent isothermal magnetization measurement at 2.0 K, as shown in Figure 6. The field-dependent magnetization of **2** shows a slight sigmoidal shape (Figure 6, inset), indicating the occurrence of a spin-flop transition. The magnetization at 50 kOe reaches only 0.76 Nβ, which is significantly lower than the expected saturated value of 10 Nβ for two Mn^{II} ions with high spin, indicating the overall AF coupling between Mn^{II} ions.

Conclusion

Two new manganese(II) azido coordination complexes with nicotinic/isonicotinic acids as the secondary bridging ligands have been structurally and magnetically charac-terized. Complex **1** is a 2D manganese(II) azido structure, but complex **2** is a 3D manganese(II) azido structure. Both complexes **1** and **2** exhibit an unprecedented topology net. Magnetic susceptibility measurements reveal dominant AF couplings in **1** and **2**. Complex **1** displays a spin-competitive behavior; however, because of spin canting, **1** has a FM-to-magnetic phase transition at the critical temperature of 6 K. Complex **2** is an antiferromagnet and exhibits a field-induced spin-flop behavior.

Supporting Information Available: X-ray crystallographic data for complexes **1** and **2** in CIF format and a file including Table S1 and Figures S1−S5. This material is available free of charge via the Internet at http://pubs.acs.org.

(24) Feng, M. L.; Prosvirin, A. V.; Mao, J. G.; Dunbar, K. R. *Chem.— Eur. J*. **2006**, *12*, 8312.